American Mineralogist, Volume 70, pages 624–629, 1985

Cation distribution studies of some ternary orthophosphates having the farringtonite structure

ANDERS G. NORD

Section of Mineralogy, Swedish Museum of Natural History
P.O. Box 50007, S-10405 Stockholm, Sweden

AND TORE ERICSSON

Department of Mineralogy and Petrology, Institute of Geology
University of Uppsala, Box 555, S-75122 Uppsala, Sweden

Abstract

Solid solutions, mainly with the composition $(Zn_{0.70}Fe_{0.25}Me_{0.05})_3(PO_4)_2$, have been analyzed by ^{57}Fe Mössbauer spectroscopy (Me = Mg, Mn, Fe, Co, Ni, Cd or Ca). The structure is isomorphous with "γ-$Zn_3(PO_4)_2$" and with farringtonite ($Mg_3(PO_4)_2$; $P2_1/n$) and contains 5- and 6-coordinated cation sites. The present qualitative results agree well with the cation ordering tendencies earlier established for binary γ-$(Zn, Me)_3(PO_4)_2$ phases. Cd^{2+} and Ca^{2+} (not earlier studied) are shown to have a preference for 6-coordination in this crystal structure. In addition, the complete cation partitioning in γ-$(Zn_{0.70}Fe_{0.20}Ni_{0.10})_3(PO_4)_2$ has been evaluated by a combination of Mössbauer spectroscopy and neutron powder diffraction. The present results show that qualitative cation ordering tendencies in binary γ-phosphates may be derived from a series of comparatively simple experiments of iron-containing ternary γ-phosphates.

Introduction

As a part of a research project on solid solutions of synthetic minerals, we have studied the distribution of Me^{2+} cations among 5- and 6-coordinated sites using "γ-$Zn_3(PO_4)_2$" (Calvo, 1963) and graftonite ((Fe, Mn, $Ca)_3(PO_4)_2$; $P2_1/c$) (Calvo, 1968) as base structures. A compound "γ-$Zn_3(PO_4)_2$" does not exist as a pure phase; it has to be stabilized by certain Me^{2+} cations and should rather be denoted γ-$(Zn, Me)_3(PO_4)_2$ (e.g., Calvo, 1963). It is isomorphous with farringtonite (DuFresne and Roy, 1961; Nord and Stefanidis, 1980) with $P2_1/n$ symmetry and containing $(M1)O_5$ polyhedra (distorted trigonal bipyramids) and rather regular $(M2)O_6$ octahedra.

We have earlier determined cation distributions in various farringtonite-type phases by use of techniques such as X-ray powder diffraction (Nord and Stefanidis, 1980), Mössbauer spectroscopy (Annersten et al., 1980), and neutron powder diffraction (e.g, Nord and Stefanidis, 1981). However, these studies were in binary systems.

We now report on a study of some ternary phases isostructural with farringtonite. The main aim has been to investigate (Zn, Fe, Me)-phases and relate the qualitative results to earlier cation distribution results on binary isostructural phases.

Experimental

Batch samples of pure $Me_3(PO_4)_2$ orthophosphates were first prepared by conventional methods (Annersten et al., 1980) for Me = Mg, Mn, Fe, Co, Ni, Cu, Zn, Cd or Ca. Ternary solid solutions were then prepared by heating appropriate mixtures in evacuated and sealed silica tubes for one month at 1070 K (800 $\pm$10°C), afterwards quenching them in cool water. The equilibrium temperature was chosen because it had been used for the binary farringtonites earlier studied by us. It was not possible to prepare the ternary phase γ-$(Zn_{0.70}Fe_{0.25}Cu_{0.05})_3(PO_4)_2$. The inability of copper to enter pure $Fe_3(PO_4)_2$-graftonite has also been noted (Nord and Ericsson, 1982).

All samples were identified by X-ray powder diffraction utilizing a Guinier-Hägg type focusing camera ($CuK\alpha_1$ radiation, λ = 1.5405Å, KCl internal standard, T = 295 K). Neutron powder diffraction data for γ-$(Zn_{0.70}Fe_{0.20}Ni_{0.10})_3(PO_4)_2$ were collected at the Studsvik R2 reactor as described by Nord (1984).

Mössbauer spectroscopy data (^{57}Fe) were recorded in transmission geometry with an electromechanical Doppler velocity generator operating at constant acceleration mode in conjunction with an ND 1200 MCA (512 channels). The contents of iron were normally less than 5 mg/cm^2 in a sample. The zero-setting and calibration of the velocity scale was done using natural iron foils (12.5 μm) at room temperature as absorbers. The analysis was made using Lorentzian lines and least squares as a norm. Since there was no indication of texture or Goldanskii–Karyagin effects in the samples (Ericsson and Wäppling, 1976), symmetrical doublets were used in the fitting procedures.

Results

X-ray powder diffraction data

All unit cell parameters ($P2_1/n$ space group symmetry, No. 14; Z = 2) are listed in Table 1. The large standard deviations of γ-$(Zn_{0.70}Fe_{0.25}Ca_{0.05})_3(PO_4)_2$ may suggest

0003–004X/85/0506–0624$02.00

Table 1. Unit cell dimensions, at 295 K, for studied samples ($P2_1/n$; Z = 2). $Zn_{0.70}Fe_{0.25}Ni_{0.05}$ stands for γ-$(Zn_{0.70}Fe_{0.25}Ni_{0.05})_3(PO_4)_2$ and so forth.

Sample	a(Å)	b(Å)	c(Å)	β(Å)	V(Å)
$Zn_{0.70}Fe_{0.30}$	7.558(2)	8.536(2)	5.042(2)	95.40(3)	323.9(2)
$Zn_{0.70}Fe_{0.25}Ni_{0.05}$	7.548(3)	8.490(3)	5.050(3)	95.12(4)	322.3(3)
$Zn_{0.70}Fe_{0.20}Ni_{0.10}$	7.540(1)	8.446(2)	5.056(1)	94.93(2)	320.8(2)
$Zn_{0.70}Fe_{0.15}Ni_{0.15}$	7.534(3)	8.411(3)	5.060(2)	94.76(3)	319.5(3)
$Zn_{0.70}Fe_{0.10}Ni_{0.20}$	7.527(3)	8.380(4)	5.063(2)	94.60(4)	318.3(3)
$Zn_{0.70}Fe_{0.05}Ni_{0.25}$	7.512(3)	8.346(5)	5.060(3)	94.54(3)	316.2(4)
$Zn_{0.70}Ni_{0.30}$ [a]	7.505(1)	8.316(1)	5.056(1)	94.48(1)	314.6(1)
$Zn_{0.70}Fe_{0.25}Ni_{0.05}$	7.548(3)	8.490(3)	5.050(3)	95.12(4)	322.3(3)
$Zn_{0.70}Fe_{0.25}Mg_{0.05}$	7.556(2)	8.498(2)	5.050(1)	95.27(2)	322.9(2)
$Zn_{0.70}Fe_{0.25}Co_{0.05}$	7.557(3)	8.517(2)	5.045(2)	95.22(3)	323.4(3)
$Zn_{0.70}Fe_{0.25}Zn_{0.05}$ [b]	7.553(3)	8.521(3)	5.039(2)	95.40(3)	322.9(3)
$Zn_{0.70}Fe_{0.25}Fe_{0.05}$ [c]	7.558(2)	8.536(2)	5.042(2)	95.40(3)	323.9(2)
$Zn_{0.70}Fe_{0.25}Mn_{0.05}$	7.564(4)	8.531(4)	5.049(2)	95.17(5)	324.5(4)
$Zn_{0.70}Fe_{0.25}Cd_{0.05}$	7.556(5)	8.550(3)	5.046(4)	95.27(5)	324.6(4)
$Zn_{0.70}Fe_{0.25}Ca_{0.05}$	7.557(8)	8.552(11)	5.049(6)	95.30(8)	324.9(8)
$Zn_{0.50}Fe_{0.10}Mg_{0.40}$	7.575(3)	9.318(4)	5.066(2)	94.78(3)	318.1(3)
$Zn_{0.50}Fe_{0.10}Co_{0.40}$	7.549(3)	8.408(5)	5.056(2)	94.58(4)	319.9(4)
$Zn_{0.50}Fe_{0.10}Co_{0.40}$	7.586(2)	9.299(4)	5.074(3)	94.20(3)	319.6(3)

The estimated standard deviations are given in parentheses.
a) Nord and Stefanidis (1981)
b,c) I.e. γ-$(Zn_{0.75}Fe_{0.25})_3(PO_4)_2$ and γ-$(Zn_{0.70}Fe_{0.30})_3(PO_4)_2$, respectively.

that the sample is somewhat inhomogeneous. The unit cell volumes are fairly well correlated with the cell contents and the cation radii as given by Shannon (1976). In particular this is obvious for the γ-$(Zn_{0.70}Fe_{0.30-x}Ni_x)_3(PO_4)_2$ phases, where V decreases linearly with the nickel contents (Ni^{2+} is the smallest cation in this study). The decrease in V is mainly due to changes in the b cell edge, while a and c change very little with the nickel contents. The same effect was noted in almost all earlier studied binary farringtonite-type phases (e.g., Nord and Stefanidis, 1980).

Mössbauer data

Typical Mössbauer spectra are shown in Figure 1. They are very similar to those of the γ-$(Zn_{1-x}Fe_x)_3(PO_4)_2$ series (Annersten et al., 1980), so the assignment is straightforward: the wide doublet represents iron at M1 (5-coordination) and the narrow doublet iron at M2 (6-coordination). Like the binary (Zn, Fe)-farringtonites, the overlap of the doublets is more pronounced at lower temperatures (77 K), so all data were recorded at room temperature (295 K). The two low-velocity peaks of the two doublets are in general well-resolved except for Cd and Ca. However, the low-velocity absorption profiles for these cations are clearly asymmetric, thus giving moderately accurate intensities. The results are summarized in Table 2. All spectra have been fitted with individual half-widths. No thickness corrections have been made in fitting the intensities of the two doublets, as the absorbers were assumed to be thin. No difference was observed in intensities I(M1)/I(M2) between two absorbers of γ-$(Zn_{0.70}Fe_{0.30})_3(PO_4)_2$ with different thicknesses (Table 2). Thus the assumption made seems to be realistic.

In all studied samples the centroid shifts CS(M1) and CS(M2) are almost independent of the composition (~1.10 and ~1.25 mm/s, respectively). The quadrupole splittings (ΔE_Q, the peak separation in a doublet) are also rather constant (~2.8 mm/s for M1 and ~1.9 mm/s for M2). Exceptions to these general tendencies include: (1) ΔE_Q(M1) is significantly smaller for the ternary phases containing the large Cd^{2+} or Ca^{2+} ions, probably due to increased distortions of the rather small 5-coordinated M1 site (cf. Ingalls, 1964). (2) In the γ-$(Zn_{0.70}Fe_{0.30-x}Ni_x)_3(PO_4)_2$ series, ΔE_Q(M2) decreases with increasing nickel contents. For x = 0, ΔE_Q(M2) is 1.95 mm/s (Annersten, Ericsson and Nord, 1980) compared to 1.24 mm/s for x = 0.25. In the binary farringtonite series γ-$(Zn_{1-x}Fe_x)_3(PO_4)_2$ and $(Mg_{1-x}Fe_x)_3(PO_4)_2$, ΔE_Q(M2) was also more sensitive to changes in the composition than ΔE_Q(M1) (Annersten et al., 1980). Although it is not obvi-

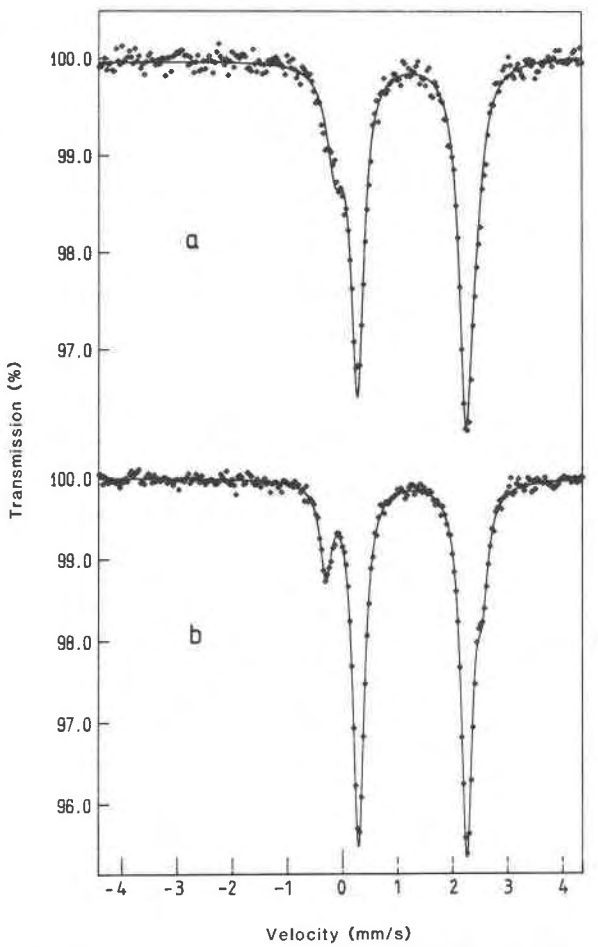

Fig. 1. Mössbauer spectra, at 295 K, of (a) γ-$(Zn_{0.70}Fe_{0.25}Cd_{0.05})_3(PO_4)_2$ and (b) γ-$(Zn_{0.70}Fe_{0.25}Co_{0.05})_3(PO_4)_2$. The continuous curves represent the computer-fitted functions and the dots are the data points.

Table 2. Mössbauer parameters for studied samples, at 295 K, together with iron site occupancies (X_{Fe}) and pseudo K_D values (K_D'). $Zn_{0.70}Fe_{0.25}Ni_{0.05}$ stands for γ-$(Zn_{0.70}Fe_{0.25}Ni_{0.05})_3(PO_4)_2$ and so forth.

Sample	M1, 5-coordination					M2, 6-coordination					
	CS[a]	ΔE_Q[b]	W[c]	Int[d]	X_{Fe}[e]	CS	ΔE_Q	W	Int	X_{Fe}	K_D'[f]
$Zn_{0.70}Fe_{0.25}Ni_{0.05}$	1.10	2.85	0.27	0.22	0.08	1.26	1.84	0.31	0.78	0.58	15.5
$Zn_{0.70}Fe_{0.20}Ni_{0.10}$	1.12	2.86	0.25	0.22	0.07	1.27	1.78	0.35	0.78	0.47	12.9
$Zn_{0.70}Fe_{0.15}Ni_{0.15}$	1.12	2.88	0.24	0.22	0.05	1.27	1.58	0.40	0.78	0.35	10.6
$Zn_{0.70}Fe_{0.10}Ni_{0.20}$	1.11	2.94	0.23	0.24	0.04	1.28	1.39	0.45	0.76	0.23	8.0
$Zn_{0.70}Fe_{0.05}Ni_{0.25}$	1.13	2.90	0.25	0.20	0.02	1.27	1.24	0.47	0.80	0.12	8.8
$Zn_{0.70}Fe_{0.25}Mg_{0.05}$	1.12	2.85	0.23	0.18	0.07	1.27	1.93	0.25	0.82	0.61	21.5
$Zn_{0.70}Fe_{0.25}Co_{0.05}$	1.12	2.85	0.25	0.19	0.07	1.28	1.97	0.25	0.82	0.61	21.2
$Zn_{0.80}Fe_{0.20}$[g]	1.12	2.80	0.33	0.16	0.05	1.25	1.93	0.29	0.84	0.50	19.6
$Zn_{0.70}Fe_{0.30}$[h]	1.11	2.81	0.25	0.18	0.08	1.26	1.95	0.27	0.82	0.74	32.9
$Zn_{0.70}Fe_{0.30}$[i]	1.11	2.78	0.26	0.18	0.08	1.26	1.97	0.26	0.82	0.74	32.0
$Zn_{0.70}Fe_{0.25}Mn_{0.05}$	1.11	2.83	0.29	0.24	0.09	1.26	1.92	0.27	0.76	0.57	13.5
$Zn_{0.70}Fe_{0.25}Cd_{0.05}$	1.12	2.55	0.39	0.27	0.10	1.26	1.98	0.30	0.73	0.55	10.5
$Zn_{0.70}Fe_{0.25}Ca_{0.05}$	1.15	2.51	0.34	0.30	0.11	1.25	1.99	0.30	0.71	0.53	9.0
$Zn_{0.50}Fe_{0.10}Mg_{0.40}$	1.11	2.89	0.26	0.39	0.06	1.26	1.46	0.39	0.62	0.19	3.7
$Zn_{0.50}Fe_{0.10}Co_{0.40}$	1.11	2.82	0.28	0.26	0.04	1.26	1.50	0.41	0.75	0.22	7.3
$Mg_{0.50}Fe_{0.10}Co_{0.40}$	1.11	2.86	0.29	0.65	0.10	1.26	1.04	0.40	0.35	0.11	1.1

a) CS = the centroid shift is relative iron metal at 295 K and measured in mm/s, precision ±0.01 mm/s.

b) ΔE_Q = the quadrupole splitting (i.e. doublet separation), ±0.02 mm/s in precision.

c) W = full width at half maximum in mm/s (±0.01 mm/s).

d) Int = intensity of the Mössbauer signal from a site (±0.01).

e) E.g. $X_{Fe}(M1)$ = fraction of iron·(number of (M1+M2)-sites)/(number of M1-sites)·Int(M1) (±0.01).

f) $K_D' = (1-X_{Fe}(M1))\cdot X_{Fe}(M2)/(1-X_{Fe}(M2))\cdot X_{Fe}(M1)$.

g) the values taken from Annersten, Ericsson and Nord (1980).

h) the iron content in the absorber is 4.7 mg/cm^2.

i) the iron content in the absorber is 1.3 mg/cm^2.

ous why ΔE_Q(M1) should be more affected than ΔE_Q(M2) when some iron is replaced by Cd or Ca while the converse is true for Ni, it may be worth mentioning that Ni^{2+} is the smallest ion and Cd^{2+} and Ca^{2+} are the largest of the cations studied here. Any site showing a composition-dependent quadrupole splitting is also more sensitive to near-neighbor effects, as noted from the broadening of the fitted doublets (Table 2). (3) Finally, in γ-$(Zn_{0.50}Fe_{0.10}Mg_{0.40})_3(PO_4)_2$, γ-$(Zn_{0.50}Fe_{0.10}Co_{0.40})_3(PO_4)_2$ and $(Mg_{0.50}Fe_{0.10}Co_{0.40})_3(PO_4)_2$ ΔE_Q(M2) is also smaller than for most other ternary farringtonites (cf. Table 2). Again this accords with the trends observed in the binary series γ-$(Zn_{1-x}Fe_x)_3(PO_4)_2$, $(Mg_{1-x}Fe_x)_3(PO_4)_2$ and $(Co_{1-x}Fe_x)_3(PO_4)_2$ (Annersten et al., 1980; Nord, Annersten, Ericsson, Sundberg and Stefanidis, to be published).

The relative intensities and the fractions of iron at M1 and M2 are given in Table 2. The values of the (Zn, Fe, Ni)-series indicate that iron and nickel have nearly the same preference for populating M2. The complete cation distribution pattern has been evaluated for γ-$(Zn_{0.70}Fe_{0.20}Ni_{0.10})_3(PO_4)_2$ (see next section).

The neutron powder diffraction data

The measured neutron intensity profile for γ-$(Zn_{0.70}Fe_{0.20}Ni_{0.10})_3(PO_4)_2$ contained 172 partly overlapping Bragg reflections ($2° \leqq \theta \leqq 40°$, $\lambda = 1.550$Å). The net intensity data were processed by means of the full-profile structure refinement technique developed by Rietveld (1969), cf. the study of γ-$(Zn_{0.70}Fe_{0.30})_3(PO_4)_2$ (Nord, 1984). The Mössbauer results given in Table 2 show that iron is distributed in such a way that $X_{Fe}(M1) = 0.07$ and $X_{Fe}(M2) = 0.47$. Accordingly, a cation distribution parameter w may be defined by means of the expression γ-$(Zn_{0.93-w}Fe_{0.07}Ni_w)_2^{M1}(Zn_{0.23+2w}Fe_{0.47}Ni_{0.30-2w})^{M2}(PO_4)_2$ ($0 \leqq w \leqq 0.15$).

The neutron scattering amplitudes were taken from the *International Tables for X-ray Crystallography, vol. IV* (1974): b(Zn) = 0.57, b(Fe) = 0.95, b(Ni) = 1.03, b(P) = 0.51 and b(O) = 0.575, all in 10^{-12} cm units. An R_I minimum, unfortunately not too distinct because of the limited fraction of heavy scatterers, was obtained at $w = 0.03 \pm 0.02$. The cation ordering in this ternary compound may thus be

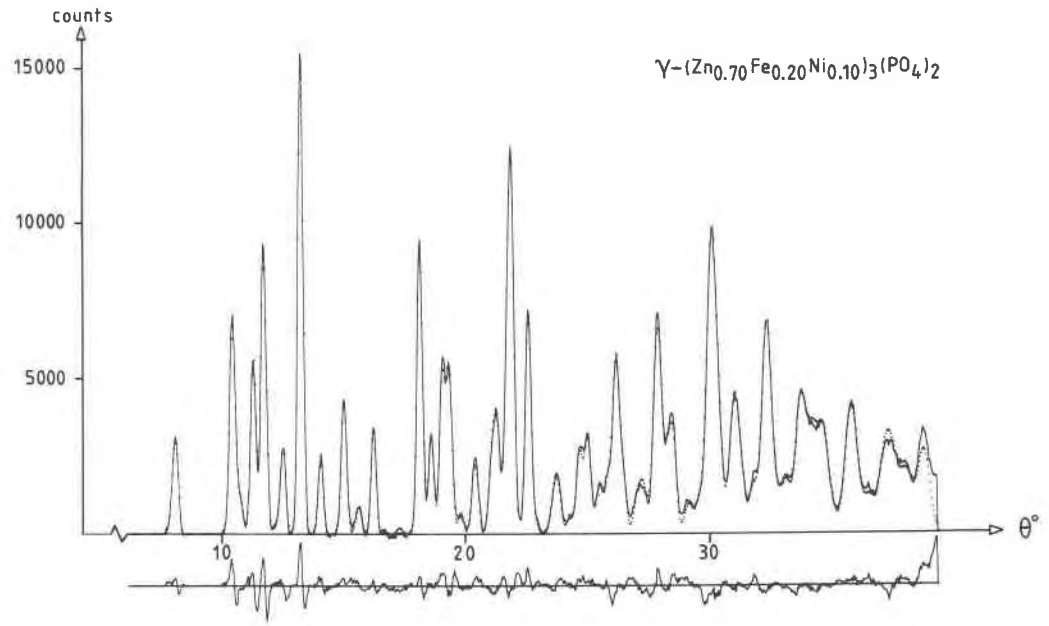

Fig. 2. The least squares fit obtained between the observed intensities (continuous curves) and calculated intensities (points) for γ-$(Zn_{0.70}Fe_{0.20}Ni_{0.10})_3(PO_4)_2$ (neutron diffraction data). The discrepancy in the fit, I_{obs}-I_{calc}, is plotted below on the same scale.

roughly described as γ-$(Zn_{0.90}Fe_{0.07}Ni_{0.03})_2^{M1}(Zn_{0.29}Fe_{0.47}Ni_{0.24})^{M2}(PO_4)_2$ (w = 0.03). The final R values (cf. Rietveld, 1969) are: $R_I = 0.044$, $R_p = 0.07$, and $R_{wp} = 0.08$. A table of the observed and calculated integrated intensities from the final refinement is available[1]. The fit obtained between the observed and calculated intensities is shown in Figure 2. The obtained atomic parameters are given in Table 3.

Discussion

The farringtonite structure is built up of somewhat distorted $(M1)O_5$ trigonal bipyramids and almost regular $(M2)O_6$ octahedra and PO_4 tetrahedra linked together to form a three-dimensional network (Fig. 3). The discussion below will mainly concern the cationic distribution among the two distinct metal sites, M1 and M2. As mentioned in the Introduction section, many cation distribution studies of binary γ-$(Zn, Me)_3(PO_4)_2$ phases have already been carried out, showing that the preference for the 5-coordinated M1 site over M2, at 1070 K, may be given by the sequence

$$Zn^{2+} \gg Co^{2+} > Fe^{2+} > Mg^{2+} > Ni^{2+} > Mn^{2+} \quad (1)$$

(cf. Nord and Stefanidis, 1980, 1981; Annersten et al., 1980).

In our ternary farringtonites, the fraction of iron at each of the two metal sites, called $X_{Fe}(M1)$ and $X_{Fe}(M2)$, is known from the Mössbauer investigations (Table 2). The three compounds γ-$(Zn_{0.50}Fe_{0.10}Mg_{0.40})_3(PO_4)_2$, γ-$(Zn_{0.50}Fe_{0.10}Co_{0.40})_3(PO_4)$ and $(Mg_{0.50}Fe_{0.10}Co_{0.40})_3(PO_4)_2$ will first be discussed. The site occupancy $X_{Fe}(M1)$ is 0.06, 0.04 and 0.10 in these three sample (same order as above), and $X_{Fe}(M2)$ is 0.19, 0.22 and 0.11. From a comparison of the (Zn, Fe, Mg)- and (Zn, Fe, Co)-samples, it is obvious that a replacement of Mg by Co leads to a decrease of $X_{Fe}(M1)$, implying that Co has a higher tendency for M1 than Mg has. Furthermore, Zn has a much higher

Table 3. Atomic parameters for γ-$(Zn_{0.70}Fe_{0.20}Ni_{0.10})_3(PO_4)_2$ (space group $P2_1/n$).

	x	y	z	B (Å^2)
M1[a)]	0.619	0.141	0.077	1.0(1)
M2[b)]	0	0	1/2	1.0(1)
P	0.198	0.194	0.032	0.8(2)
O(1)	0.050	0.132	0.823	0.5(1)
O(2)	0.125	0.197	0.303	0.5(1)
O(3)	0.256	0.357	0.940	0.5(1)
O(4)	0.361	0.078	0.053	0.5(1)

The numbers within parentheses for the thermal parameters represent estimated standard deviations referring to the uncertainty in the decimal.

a) The determined cation occupancy for M1 is $Zn_{0.90}Fe_{0.07}Ni_{0.03}$ *(see text).*

b) The determined cation occupancy for M2 is $Zn_{0.29}Fe_{0.47}Ni_{0.24}$ *(see text).*

The estimated standard deviations for all positional parameters are ±0.001.

[1] To obtain a copy of this table, order Document AM-85-266 from the Business Office, Mineralogical Society of America, 2000 Florida Avenue, N.W., Washington, D.C. 20009. Please remit $5.00 in advance for the microfiche.

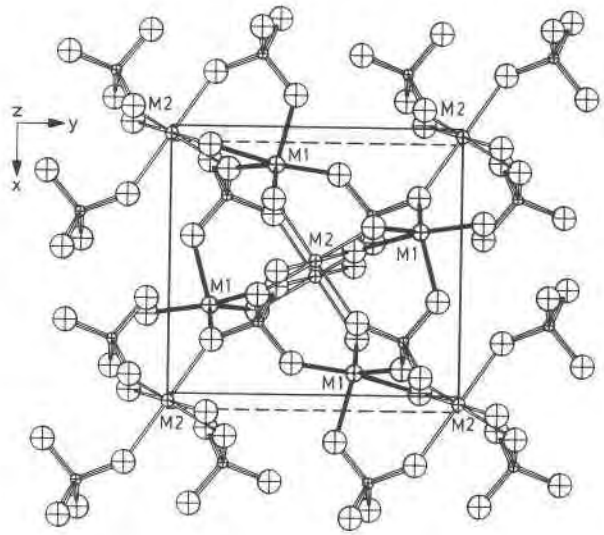

Fig. 3. ORTEP (Johnson, 1965) plot picture of the crystal structure of farringtonite.

tendency than Mg to occupy M1, which follows from a comparison of the (Zn, Fe, Co)- and (Mg, Fe, Co)-samples. Although the stoichiometry is not quite the same, the (Zn, Fe, Mg)- and (Mg, Fe, Co)-samples may also be compared, showing that Zn has a much higher tendency than Co to occupy M1. This gives the following M1 site preference order:

$$Zn^{2+} \gg Co^{2+} > Mg^{2+} \qquad (2)$$

which agrees with sequence (1). Accordingly, simple experiments performed on ternary phases may give a qualitative picture of the cation ordering tendencies, although the complete cation partitionings are not known.

The γ-$(Zn_{0.70}Fe_{0.30-x}Ni_x)_3(PO_4)_2$ solid solutions will be discussed in some detail. The complete cation distributions have been determined for three compositions, with the following results:

$$\gamma\text{-}(Zn_{0.92}Fe_{0.08})_2^{M1}(Zn_{0.26}Fe_{0.74})^{M2}(PO_4)_2 \qquad (x = 0)$$

$$\gamma\text{-}(Zn_{0.90}Fe_{0.07}Ni_{0.03})_2^{M1}(Zn_{0.29}Fe_{0.47}Ni_{0.24})^{M2}(PO_4)_2 \qquad (x = 0.10)$$

$$\gamma\text{-}(Zn_{0.93}Ni_{0.07})_2^{M1}(Zn_{0.24}Ni_{0.76})^{M2}(PO_4)_2 \qquad (x = 0.30)$$

The result for x = 0 is taken from Annersten, Ericsson and Nord (1980), x = 0.10 from this study, and x = 0.30 from Nord and Stefanidis (1981).

The preference to occupy M1 is clearly highest for Zn. The preferences for Fe and Ni to occupy M1 are obviously not very different. Thus one may assume that the populations of Zn, Fe and Ni at M1 and M2 are linear functions of x. On the basis of this assumption, the site populations have been extrapolated and given in Figure 4. The average metal–oxygen distances obtained for γ-$(Zn_{0.70}Fe_{0.20}Ni_{0.10})_3(PO_4)_2$ are reasonable, namely 2.06(2)Å for M1 and 2.13(1)Å for M2 (Table 4). The corresponding

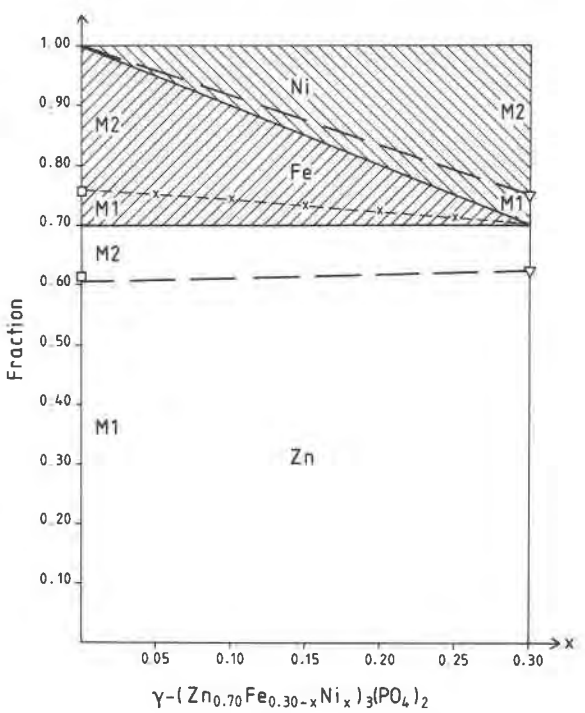

Fig. 4. The amounts of zinc, iron and nickel entering the M1- and M2-sites as a function of the composition x in γ-$(Zn_{0.70}Fe_{0.30-x}Ni_x)_3(PO_4)_2$. The dashed lines are drawn under the assumption of linear variations (see text). The unshaded area represents Zn, the right-slanted Fe and the left-slanted Ni. □ = Annersten, Ericsson and Nord (1980), Δ = Nord and Stefanidis (1981), x = this study. (The fraction of M1 sites compared to (M1 + M2) is 2/3.)

values are 2.06(2)Å and 2.17(1)Å in γ-$(Zn_{0.70}Fe_{0.30})_3(PO_4)_2$ (Nord, 1984) and 2.04(2)Å and 2.12(1)Å in γ-$(Zn_{0.70}Ni_{0.30})_3(PO_4)_2$ (Nord and Stefanidis, 1981).

In Table 2, a pseudo-distribution coefficient K'_D has been defined as:

$$K'_D = (X_{Zn+Me}(M1) \cdot X_{Fe}(M2))/(X_{Zn+Me}(M2) \cdot X_{Fe}(M1))$$

where $X_{Fe}(M1)$ denotes the fraction at M1 occupied by Fe and so on. The Mössbauer results of the various

Table 4. Some interatomic distances (Å) and angles (°) in γ-$(Zn_{0.70}Fe_{0.20}Ni_{0.10})_3(PO_4)_2$.

M1 - O(1)	2.36(2)	M2 - O(1)	(x2)	1.99(1)
M1 - O(2)	1.95(2)	M2 - O(2)	(x2)	2.20(1)
M1 - O(3)	2.03(2)	M2 - O(3)	(x2)	2.19(1)
M1 - O(4)	2.01(2)	M2 - O mean		2.13(1)
M1 - O(4')	1.97(2)			
M1 - O mean	2.06(2)	O(1) - P - O(2)		108.9(6)
		O(1) - P - O(3)		107.5(6)
P - O(1)	1.56(1)	O(1) - P - O(4)		110.4(6)
P - O(2)	1.52(1)	O(2) - P - O(3)		113.0(6)
P - O(3)	1.54(1)	O(2) - P - O(4)		107.1(6)
P - O(4)	1.57(1)	O(3) - P - O(4)		109.9(6)
P - O mean	1.55(1)	O - P - O mean		109.5(6)

γ-$(Zn_{0.70}Fe_{0.25}Me_{0.05})_3(PO_4)_2$ phases have been compared by means of these K'_D-values. Since a low K'_D value accords with a low tendency of Me^{2+} to occupy the 5-coordinated M1 site, the following preference order for M1 can be established:

$$Co^{2+}, Mg^{2+} > Ni^{2+} > Mn^{2+} > Cd^{2+} > Ca^{2+} \quad (3)$$

This agrees well with sequence (1), although this did not include the two largest cations (Cd^{2+} and Ca^{2+}) which can only be incorporated in minute amounts in zinc orthophosphate (Brown and Hummel, 1963; Kreidler and Hummel, 1967). The advantage of incorporating iron in binary compounds to form ternary phases accessible to Mössbauer spectroscopy is obvious. The position of Fe^{2+} in sequence (3), valid for ternary γ-phosphates, is derived from the intensities in Table 2 for $Zn_{0.70}Fe_{0.30}$, i.e. $Zn_{0.70}Fe_{0.25}Fe_{0.05}$ phosphates. The comparison gives approximately the same tendency for Fe, Mg and Co to occupy M1.

Furthermore, the sequences (2) and (3) for ternary phosphates agree with sequence (1), valid for binary phosphates. Thus it seems natural to combine (1), (2) and (3) to get the preferential order to occupy the 5-coordinated M1 site at 1070 K:

$$\begin{array}{cccccccc} Zn^{2+} \gg & Co^{2+} > & Fe^{2+} > & Mg^{2+} > & Ni^{2+} > & Mn^{2+} > & Cd^{2+} > & Ca^{2+} \\ 0.74 & 0.75 & 0.78 & 0.72 & 0.69 & 0.83 & 0.95 & 1.00 \end{array} \quad (4)$$

The effective ionic radii, in Ångström units (Shannon, 1976), are given below the elements. K_D values of binary γ-phases containing neither zinc nor iron have been determined earlier, also showing this sequence to have a general validity (cf. Nord and Stefanidis, 1980, 1981). The position of Zn^{2+} is in accordance with crystal chemistry: the "γ-$Zn_3(PO_4)_2$" phase is not stable unless other divalent cations with preference for the M2 site are incorporated in the structure. The position of the small Ni^{2+} ion in sequence (4) reflects its tendency to occupy highly symmetrical octahedral sites and is in agreement with theory (Burns, 1970). As the M2 site is larger than M1, it is tempting to suggest that the positions in sequence (4) of the largest cations are mainly controlled by size effects. However, our earlier cation distribution studies have shown that crystal field effects are also very important (cf. Nord and Stefanidis, 1981; Nord and Ericsson, 1982). The present study shows that ^{57}Fe Mössbauer spectroscopy on iron-containing ternary solid solutions may give useful information on qualitative cation preferences even if the complete cation distribution pattern is not obtained. A moderately accurate evaluation of the complete pattern can be mastered by a combination of Mössbauer spectroscopy and a diffraction technique.

Acknowledgments

It is a great pleasure to thank professor Hans Annersten (University of Uppsala) for many valuable discussions concerning this work. Many thanks are also due to Dr Roland Tellgren (University of Uppsala) for his helpfulness during the collection of the neutron diffraction data, and to Miss Kersti Gløersen for her skilful typing of the manuscript.

This work has received financial support from the Swedish Natural Science Research Council (NFR).

References

Annersten, H., Ericsson, T. and Nord, A. G. (1980) The cation ordering in iron-containing zinc and magnesium orthophosphates determined from Mössbauer spectroscopy. Journal of the Physics and Chemistry of Solids, 41, 1235–1240.

Brown, J. J. and Hummel, F. A. (1963) Phase equilibria and manganese-activated luminescence in the system $Zn_3(PO_4)_2$-$Cd_3(PO_4)_2$. Journal of the Electrochemical Society, 110, 1218–1223.

Burns, R. G. (1970) Mineralogical Applications of Crystal Field Theory. Cambridge University Press, Cambridge, England.

Calvo, C. (1963) The crystal structure and luminescence of γ-zinc orthophosphate. Journal of the Physics and Chemistry of Solids, 24, 141–149.

Ericsson, T. and Wäppling, R. (1976) Texture effects in 3/2–1/2 Mössbauer spectra. Journal de Physique, Colloque C6, 37, 719–723.

DuFresne, E. R. and Roy, S. K. (1961) A new phosphate mineral from the Springwater pallasite. Geochimica et Cosmochimica Acta, 24, 198–205.

Ingalls, R. (1964). Electric-field gradient tensor in ferrous compounds. Physical Review, 133A, 787–795.

International Tables for X-ray Crystallography (1974). Vol. IV. Kynoch Press, Birmingham.

Johnson, C. K. (1965) ORTEP: a Fortran thermal-ellipsoid plot program for crystal structure illustrations, AEC Accession No. 33516, Oak Ridge National Laboratory, Tennessee.

Kreidler, E. R. and Hummel, F. A. (1967) Phase equilibria in the system $Ca_3(PO_4)_2$–$Zn_3(PO_4)_2$. Inorganic Chemistry, 6, 524–528.

Nord, A. G. (1984) Use of the Rietveld technique for estimating cation distributions. Journal of Applied Crystallography, 17, 55–60.

Nord, A. G. and Ericsson, T. (1982) Cation distributions in $(Fe_{1-z}Me_z)_3(PO_4)_2$ graftonite-type solid solutions determined by Mössbauer spectroscopy. Zeitschrift für Kristallographie, 161, 209–224.

Nord, A. G. and Stefanidis, T. (1980) The cation distribution between five- and six-coordinates sites in some (Mg, *Me*)$_3(PO_4)_2$ solid solutions. Materials Research Bulletin, 15, 1183–1191.

Nord, A. G. and Stefanidis, T. (1981) A neutron diffraction study of γ-$(Zn_{0.70}Ni_{0.30})_3(PO_4)_2$. Acta Crystallographica, B37, 1509–1511.

Rietveld, H. M. (1969) A profile refinement method for nuclear and magnetic structures. Journal of Applied Crystallography, 2, 65–71.

Shannon, R. D. (1976) Revised effective ionic radii and systematic studies on interatomic distances in halides and chalcogenides. Acta Crystallographica, A32, 751–767.

Manuscript received, May 14, 1984;
accepted for publication, December 27, 1984.